Full Title: Androgen-regulated microRNA-135a decreases prostate cancer cell migration and invasion through down-regulating ROCK1 and ROCK2

Running Title: Androgen-induced miR-135a targets ROCK1 and ROCK2

Authors: Auriane KROISS[1], Séverine VINCENT[1], Myriam DECAUSSIN-PETRUCCI[1,2,3], Emmanuelle MEUGNIER[4], Jean VIALLET[5], Alain RUFFION[1,2,6], Frédéric CHALMEL[7], Jacques SAMARUT[1,2,8] and Nathalie ALLIOLI[1,9]

Authors Affiliations:

[1]Université de Lyon, Ecole Normale Supérieure de Lyon, Université Lyon 1, IGFL, France.

[2]Faculté de Médecine Lyon-Sud, Université Lyon 1, France.

[3]Service d'Anatomie et de Cytologie Pathologiques, Hôpital Lyon-Sud, Hospices Civils de Lyon, France.

[4]Laboratoire CarMen, INSERM U1060, INRA1362, Université Lyon 1, Faculté de Médecine Lyon-Sud, France.

[5]*In Ovo*, Institut Albert Bonniot, CRI INSERM/UJF U823, Université de Grenoble, France.

[6]Service d'Urologie, Hôpital Lyon-Sud, Hospices Civils de Lyon, France.

[7]GERHM, INSERM U1085-Irset, Université Rennes 1, France.

[8]UMOMT, Hôpital Lyon-Sud, Hospices Civils de Lyon, France.

[9]ISPB, Université de Lyon, France.

Correspondence: Jacques SAMARUT (jacques.samarut@ens-lyon.fr), Nathalie ALLIOLI (nathalie.allioli@univ-lyon1.fr); Institut de Génomique Fonctionnelle de Lyon, 32-34 avenue Tony Garnier, 69007 Lyon, FRANCE.

Abstract

Androgen signaling, *via* the androgen receptor (AR), is crucial in mediating prostate cancer initiation and progression. Identifying new downstream effectors of the androgens/AR pathway will allow a better understanding of these mechanisms and could reveal novel biomarkers and/or therapeutic agents to improve the rate of patient survival.

We compared the microRNA expression profiles in androgen-sensitive LNCaP cells stimulated or not with 1 nM R1881, by performing a high-throughput RT-qPCR and found that miR-135a was up-regulated. After androgen stimulation, we showed that AR directly activates the transcription of *miR-135a2* gene by binding to an androgen response element in the promoter region. Our findings identify miR-135a as a novel effector in androgens/AR signaling.

Using xenograft experiments in chick embryos and adult male mice, we showed that miR-135a overexpression decreases *in vivo* invasion abilities of prostate PC-3 cells. Through *in vitro* wound healing migration and invasion assays, we demonstrated that this effect is mediated through down-regulating ROCK1 and ROCK2 expression, two genes that we characterized as miR-135a direct target genes.

In human surgical samples from prostatectomy, we observed that miR-135a expression was lower in tumoral compared to paired adjacent normal tissues, mainly in tumors classified with a high Gleason score (≥ to 8). Moreover, miR-135a expression is lower in invasive tumors, showing extraprostatic extension, as compared to intraprostatic localized tumors. In tumor relative to normal glands, we also showed a more frequently higher ROCK1 protein expression determined using a semi-quantitative immunohistochemistry analysis. Therefore, in tumor cells, the lower miR-135a expression could lead to a higher ROCK1 protein expression which could explain their invasion abilities. The highlighted relationship between

miR-135a expression level and the degree of disease aggressiveness suggests that miR-135a may be considered as a prognostic marker in human prostate cancer.

Introduction

Androgens play a pivotal role in initiation and progression of prostate cancer (PCa) (1-3). They function mainly by regulating target gene expression *via* the androgen receptor (AR) (4). AR acts as a ligand regulated transcription factor, which binds androgen response elements (ARE) in targeted genes. Localized PCa can be treated either by surgical resection or radiation therapy. For advanced or metastatic PCa, first-line therapeutic strategy is androgen deprivation associated with AR antagonists (5). Despite a good initial response, the disease progresses to a castration resistant prostate cancer (CRPC) (6, 7), which has limited therapeutic options and poor prognosis. A current challenge in PCa management is to understand the molecular mechanisms controlling disease progression (8).

MicroRNAs (miRs) are small non-coding RNAs, acting as negative post-transcriptional regulators of protein-coding gene expression (9). MiRs interact by imperfect binding to specific-sequence located within the 3' untranslated region (3'UTR) of targeted mRNAs, directing mRNA inactivation and/or translational repression. MiRs function as oncogenes (10) or tumor-suppressor genes (11, 12), can promote metastases spreading to distant sites (13, 14) and their deregulation is a common feature of human cancers initiation and progression (15). Moreover, miRs are already entering the clinic as diagnostic/prognostic indicators for patient stratification and as therapeutic strategies (12).

Among deregulated miRs in PCa (16-19), some are under AR regulation (20-23). However, constructive analyses of the molecular mechanisms underlying such a regulation are lacking. MiRs working as effectors of androgens signaling might be biomarkers of prostatic tumor development, as well as therapeutic targets for innovative therapies.

Here, we identified miR-135a as an androgen up-regulated miR and investigated its mechanisms of action in PCa cells. Finally, we analyzed miR-135a expression in surgical samples and explored correlation with PCa progression.

Results

Identification of miR-135a as an androgen induced microRNA.

To identify new androgen-regulated miRs in prostate cells, we performed a high-throughput RT-qPCR analysis (**Supplementary data 1**) and compared the expression level of 377 microRNAs in prostate androgen-sensitive LNCaP cells cultured for 2, 8, 24 and 48 hours in the presence or absence of 1 nM R1881. We observed that nine miRNAs were statistically up-regulated by androgens but only five (miR-135a, -135b, -193a-3p, -29a and -486-5p) were validated in a reproducible manner by RT-qPCR individual assays, in biological replicates. Finally, due to the greatest induction of its expression after androgen treatment, miR-135a was chosen for further investigation.

As shown in **Figure 1A,** miR-135a expression increased after 8 h of androgen treatment (2 fold over vehicle) to reach a 10 fold increase after 24 h. Moreover, R1881-induced miR-135a expression was reduced (-76.5%) in the presence of bicalutamide, an AR antagonist (**Figure 1B**) and also following si-AR transfection (-70%; **Figure 1C**), strongly suggesting the involvement of AR in androgen-mediated regulation of miR-135a expression. Finally, the induction of miR-135a expression by R1881 was not affected in the presence of cycloheximide (**Figure 1D**), suggesting that the androgen-mediated miR-135a expression was directly induced by AR, without the requirement of intermediate protein factor synthesis.

A similar androgen-induced miR-135a expression was observed, after 24 h of R1881 treatment, in MOP and 22Rv1 cells, two other androgen-responsive prostate cell lines (22.8 and 4.16 fold increase, respectively).

AR regulates *miR-135a2* gene expression at transcriptional level.

The mature miR-135a could be produced by two *miR-135a* genes in the human genome. *MiR-135a1* and *miR-135a2* are localized on chromosome 3 and 12, respectively. We analysed the expression of both genes after androgenic treatment by quantifying the amount of each pri-miR **(Figure 1E)** and observed that only pri-miR-135a2 expression was increased.

A kinetic study revealed a rapid increase of pri-miR-135a2 expression within 1 h after androgen treatment. The fold induction increased until 12 h and then decreased while androgenic induction of mature miR-135a expression started after 6 h and rose until 24 h (**Figure 1F**).

These data strongly suggest that the increased amount of mature miR-135a following androgen stimulation resulted from transcriptional activation of the *miR-135a2* gene.

Mechanisms of regulation of the *miR-135a2* gene transcription.

MiR-135a2 sequence is localized in an intron of the non-coding *RMST* gene (MI0000453, http://www.mirbase.org). However, this gene is not expressed in LNCaP cells (unpublished data), suggesting that *miR-135a2* gene has its own transcriptional regulatory sequences. By 5'RACE in LNCaP cells, we identified a transcription start site located 554 bp upstream of the first base of the pre-miR-135a2, which matches with the beginning of an Expressed Sequence Tag (EST, gb CA311800) (**Figure 2A**).

As miR-135a was transcriptionally regulated by androgens *via* AR, functional AREs were searched within the *miR-135a2* gene region. Using MatInspector software, we identified seven putative AREs in the 10 kb region upstream of the pre-miR-135a2 (**Figure 2B**). Transcriptional activities of three ARE-containing regions (-8800/-7600; -6740/-5500; -1380/0) were tested in luciferase reporter assays. Only the construct containing the -6740/-5500 fragment mediated activation (3.6 fold) of luciferase gene expression in response to

androgens (**Figure 2C**). This construct contains four potential AREs, termed ARE-2 to ARE-5. Because the ARE-2 (caagtacagcttGTTCtcc), located at -5605 bp, is very close to the ARE consensus sequence (4), it was mutated (caagtaAagcttTTTCtcc) to check its role in androgen induction. As shown in **Figure 2C**, the induction of luciferase expression by R1881 was totally abolished by the mutation. Using chromatin immunoprecipitation (ChIP) with an AR specific antibody, we demonstrated in LNCaP cells a 4 fold increase of AR binding after R1881 stimulation onto the region containing ARE-2 (**Figure 2D**). Finally, these data suggest that *miR-135a2* is a direct AR target gene.

miR-135a directly targets ROCK1 and ROCK2.

To explore the biological role of miR-135a, we searched for its putative target mRNAs. We performed a gene expression analysis in LNCaP cells overexpressing miR-135a versus cells transfected with miR negative control (miR-NC), using pangenomic microarrays. Details regarding the arrays are described in **Supplementary data 2**. In LNCaP cells overexpressing miR-135a, we identified 123 deregulated genes, mainly involved in cellular movement, cellular assembly/organization and cell morphology (Gene Ontology analyses), suggesting that miR-135a overexpression might affect these biological functions. Among the deregulated genes, 67 were down-regulated, 39 of which are potential direct targets containing complementary sequences of miR-135a seed box in their 3'UTR, as predicted by TargetScan. *ROCK1*, which encodes a Rho-associated kinase, belongs to these potential direct target genes. The second member of the ROCK family, *ROCK2*, (although not being listed as differentially expressed gene in microarray statistical analysis because of a hybridization defect on one of the two chip replicates), is implicated in same pathways and is also predicted to be a potential target gene (TargetScan). So, we focused our further analysis on *ROCK1* and *ROCK2*, as potential targets of miR-135a.

We confirmed the effect of miR-135a overexpression on the down-regulation of ROCK1 and ROCK2 expression, at mRNA and protein levels, by RT-qPCR and western blot analyses, respectively. LNCaP cells transfected with miR-135a mimics showed nearly 50% decrease in ROCK1 and ROCK2 mRNA levels (**Figure 3A**) and a dramatic decrease of ROCK1 and ROCK2 protein levels (up to 96% and 80%, respectively), as compared to control cells (**Figure 3B)**. Next, we generated plasmids containing the 3'UTR of ROCK1 or ROCK2 downstream of a luciferase gene (wt 3'UTR) and similar plasmids in which the sequences recognized by the miR-135a were deleted (mut 3'UTR) (**Figure 3C**). In HeLa cells co-transfected with miR-135a mimics and wild type constructs, we observed a decrease in the luciferase activities (-57% and -32% for ROCK1 and ROCK2 constructs, respectively), as compared to pmirGLO empty vector (**Figure 3D)**. In contrast, the expressions of the luciferase gene from mutant constructs were not affected by miR-135a overexpression. These data then revealed a direct interaction between miR-135a and 3'UTR of ROCK1 and ROCK2 mRNAs. Altogether, these data confirm that ROCK1 and ROCK2 are specific direct targets of miR-135a.

Androgens/AR signaling down-regulates ROCK1 and ROCK2 through miR-135a.

In R1881-treated LNCaP cells, in which miR-135a expression was increased, we observed a strong decrease of ROCK1 and ROCK2 protein amounts (-74% and -65%, respectively; **Figure 3E**). The R1881-induced depletion of ROCK1 protein expression was blocked after a miR-135a inhibitor treatment (**Figure 3E**), suggesting that androgens down-regulate the expression of ROCK genes through miR-135a.

miR-135a inhibits *in vitro* cell migration and invasion by targeting ROCK1 and ROCK2.

ROCK1 and ROCK2 proteins have been implicated in different cellular processes like migration and invasion. We then wondered whether miR-135a overexpression might modulate these cellular properties. We analysed the effect of miR-135a on cell behaviour using PC-3 prostate cells, which are endowed with migratory and invasiveness properties.

In a wound healing migration assay, we observed that the speed of wound closure was significantly decreased in PC-3 cells overexpressing miR-135a (**Figure 4A**), suggesting that miR-135a has an anti-migratory action. In parallel, we artificially lowered the expression of the ROCK1 and ROCK2 proteins by co-transfecting siROCK1 and siROCK2 (siROCK1/2) or treating the cells with Y-27632, a chemical inhibitor of the ROCK kinases. These treatments also decreased cell migration, supporting the role of ROCK1 and ROCK2 in mediating the anti-migratory effect of miR-135a. To confirm this hypothesis, we co-expressed miR-135a and ROCK1 in PC-3 cells, which then recovered their migratory properties as compared to cells expressing miR-135a only. A further confirmation was brought when we looked at the phenotype of migrating cells. Cells transfected with miR-135a appeared elongated with multiple protrusions (**Figure 4B**), like siROCK1/2 transfected cells. Interestingly, forcing the expression of exogenous ROCK1 in cells overexpressing miR-135a restored a normal cell phenotype. All these data support then strongly the role of ROCK proteins in mediating the effects of miR-135a on cell migration.

We further analysed the role of miR-135a in cell invasiveness. As shown in **Figure 4C**, overexpression of miR-135a as well as siROCK1, siROCK2 or treatment with Y-27632 strongly decreased cell invasiveness. Here again, inhibition of cell invasiveness by miR-135a was abrogated by overexpressing ROCK1.

miR-135a overexpression inhibits *in vivo* tumoral cell invasion, in chick embryo and adult mouse.

To confirm the *in vitro* anti-invasiveness action of miR-135a, we investigated its effect *in vivo*, by using xenograft tumor experiments, in chick embryo and adult male murine models. We used PC-3 cells stably overexpressing either miR-135a or the miR-Null as control.

A first xenograft experiment was performed by grafting modified PC-3 cells onto the chorioallantoic membrane (CAM) of 10 days chick embryos. At embryonic day 19, the developed tumors were recovered from the upper CAM and weighted. We did not observe any difference in embryo survival (80 *versus* 77.2%) or in tumor growth between the two groups of grafted embryos. We next counted the number of nodules in the lower CAM to assess the ability of the tumors to disseminate. An average of 3.071 ($\pm$ 1.016) nodules were counted in the lower CAM of PC-3 miR-Null grafted embryos, while an average of only 0.852 ($\pm$ 0.718) nodules was counted in the lower CAM of PC-3 miR-135a grafted embryos (**Figure 5A**), suggesting that miR-135a inhibits the invasion ability of tumors.

A second xenograft experiment was performed by injecting modified PC-3 cells subcutaneously into SCID mice. Interestingly, we observed, after 6 weeks, a strong difference in the localization of developed tumors between the two groups. All tumors that developed from PC-3 miR-135a cells showed a restricted subcutaneous localization and did not cross the peritoneum to invade the abdominal cavity. In contrast, all the tumors developed from PC-3 miR-Null showed an evident penetration of the peritoneum. Representative images are shown in **Figure 5B**.

These *in vivo* experiments clearly demonstrated that overexpressing miR-135a in the invasive PCa PC-3 cells efficiently inhibited their dissemination from the initial tumor, suggesting that miR-135a disrupts *in vivo* cell migration and invasion processes.

miR-135a expression decreases in tumoral compared to adjacent normal prostate tissues and with prostate cancer progression.

To investigate the clinical value of miR-135a in PCa, we determined miR-135a expression level in 56 tumors and pair-matched adjacent normal tissues from prostatectomy (**Supplementary Tables 2-3**), by RT-qPCR.

We found that miR-135a expression was significantly lower ($p<0.0001$) in tumor tissues than in paired normal tissues (**Figure 6A**). We then analyzed the relation between miR-135a expression and pathological grading. We observed a lower expression of miR-135a relative to paired normal tissue, in all the tumors classified with a high Gleason score (≥ to 8), compared to tumors with Gleason score ≤ to 7 (**Figure 6B**). We finally observed a significant decrease in miR-135a expression in invasive extraprostatic tumors (pT3a and b stages) as compared to intraprostatic localized tumors (pT2c stage) (**Figure 6C**), even if we could not separate seminal vesicle dissemination (pT3b stage) from non-seminal dissemination (pT3a stage) in extraprostatic group (**Figure 6C**). Therefore, the miR-135a expression level was inversely correlated with the pathological staging, precisely between localized and invasive tumors types.

All these data suggest a decrease in miR-135a expression during PCa progression.

ROCK1 protein expression is higher in tumoral compared to normal prostate glands.

We next checked whether the ROCK1 expression might reflect miR-135a expression in prostate tumors. First, we determined ROCK1 mRNA expression level, by RT-qPCR, in the same samples in which we had previously determined miR-135a expression level. We did not observe any correlation between ROCK1 mRNA and miR-135a expression levels in these samples. Finally, immunohistochemistry analysis was performed on prostate sections containing both normal and tumor glands, from each of the 56 patients of the same cohort.

ROCK1 protein was revealed in both basal and glandular cells of glandular epithelium, and we observed more frequently a higher staining, corresponding to a higher ROCK1 protein expression, in tumor glands than in adjacent normal prostatic glands (**Figure 6D**). A semi quantitative analysis revealed a higher percentage of "high level" staining in tumor glands (29%) relative to normal glands (13%) (**Figure 6E**). In conclusion, ROCK1 protein expression seemed to be more frequently higher in tumor prostate tissue in which miR-135a expression was decreased.

Discussion

In the present study, we investigated the miRNome of LNCaP cells after androgenic stimulation, using microRNA Low Density Array profiling. We identified five significantly androgen up-regulated miRNAs, among which miR-135a showed the highest induction by androgens. Mir-193a-3p and miR-29a were previously reported as androgen induced miRs in LNCaP cells (20, 24) confirming the relevance of our approach.

The expression of several miRs has been previously shown to be modulated by androgens in PCa cells (20, 21, 24-26). However, except for few of them (miR-21 (20); miR-27a (22); miR-32 and miR-148 (21)), the mechanisms of such androgenic regulation remain largely unexplored. A previously described ChIP-seq study identified an AR binding site in miR-135a gene without specifying its localization or its functionality (21). In our study, we have shown that miR-135a androgen-mediated expression results from AR binding on a functional ARE upstream of the *miR-135a2* gene.

To explore the biological effects of miR-135a in prostate cells, we overexpressed miR-135a in LNCaP cells and performed transcriptomic and *in silico* analyses. We identified 39 down-regulated genes whose 3'UTR contains a complementary sequence to the miR-135a seed box. We focused on genes implicated in cell movement/morphology and organization processes (KCNMA1, KIF23, LCP1, NPC1, ROCK1 and ROCK2) and validated their microarray expression data by RT-qPCR analyses. For two of them, ROCK1 and ROCK2, we demonstrated that miR-135a interacts with their 3'UTR and down-regulates their expression, at mRNA and protein levels, attesting that ROCK1 and ROCK2 are miR-135a direct targets. ROCK1 and ROCK2 are implicated in actin cytoskeleton organization and actomyosin interaction, controlling thereby cell motility, adhesion and contraction (27, 28). Inhibition of

ROCKs has been shown to decrease *in vitro* migration and invasion ((29) and our present data) and *in vivo* dissemination of the invasive PC-3 cells (29).

Taking these observations in account, we tested whether miR-135a could modulate these cellular processes in prostate cells. Using xenograft experiments, we showed that miR-135a overexpression inhibited *in vivo* PC-3 cell invasion in chick embryo and adult mouse.

In addition, we demonstrated that the effect of miR-135a in decreasing PC-3 cell migration and invasion was mediated through ROCKs down-regulation. Similar results were obtained in HeLa cells (data not shown; (30)) and in gastric cells where miR-135a ability to suppress cell migration/invasion was also described to be mediated through ROCK pathway (31). In contrast, miR-135a has been reported to promote cell migration/invasion in other cell types like breast, colorectal and cervical cancer cells by targeting HOXA10 (32), MTSS1 (33) and SIAH1 (34) mRNAs respectively.

We next investigated the clinical significance of miR-135a expression in PCa samples. We observed that miR-135a expression level was significantly reduced in tumoral compared to pair-matched normal tissues, especially in patients with a high pathological grade, suggesting that miR-135a could be implicated in PCa progression. Moreover, miR-135a expression level decreases in invasive extraprostatic tumors (pT3) compared to intraprostatic localized tumors (pT2). As patients classified in pT3 stages relapse more quickly after chirurgical treatment (less than 5 years) than patients classified in pT2 stages, miR-135a might also be considered as a prognostic marker in PCa. We showed that miR-135a expression in androgen dependent (*AD*) LNCaP cell line is higher than in its androgen independent (*AI*) C4-2B and MOP sublines (data not shown); in the same way Ma et al have shown that miR-135a expression is lower in *AI* LNCaP-LNO *versus* LNCaP cells (35). As suggest by Wang et al (36), by using a computational approach combining microarray data, miR-135a could regulate the expression of genes influencing the progression of androgen-dependent to androgen-independent PCa.

Most of miRs up-regulated by androgens function as oncogenes, whereas miRs repressed by androgens function as tumor suppressors (20-22, 37-39). Interestingly, miR-135a expression is up-regulated by androgens and down-regulated in PCa cells, following a pattern identical to miR-29a (20, 40) and miR-Let7-c (41, 42). Moreover, miR-135a decreases the invasiveness of PC-3 cells, like miR-101 another androgen up-regulated miR (43).

In tumor relative to normal glands, we showed a lower expression of miR-135a and a more frequently higher ROCK1 protein expression. As miR-135a expression level decreased, from low to high grade PCa, it could lead to an increase of ROCK1 expression and could explain an increase of tumor cell migration, invasion and metastasis dissemination.

Links have been reported between androgens, AR and Rho/ROCK pathways: expression of RhoA, ROCK1 and ROCK2 are linked to AR expression level (44), androgens induce activation of RhoA and its translocation into the plasma membrane (45), RhoA has been recently identified as a direct AR-targeted gene (46) and Rho signaling has been involved in functional activation of AR (47). Interestingly, we have identified a novel way mediating the effects of androgens *via* AR in Rho signaling, through the regulation of miR-135a expression and its targets ROCK1/ROCK2.

In conclusion, studying miR-135a and the whole panel of its target genes might identify novel potential biomarkers and alternative therapeutic strategies for survival improvement of patients with PCa.

Materials and Methods

Cells. Human prostate (LNCaP and PC-3) and HeLa cells were cultured, as indicated by the ATCC. We generated PC-3 cells stably transfected with a pEGP-miR-Null vector (Cell biolabs) or a pEGP-miR-135a2 vector expressing a mature miR-135a.

Androgen treatment. LNCaP cells were deprived of steroid during 48 h in phenol red-free RPMI 1640 medium supplemented with 5% charcoal filtered serum and treated with 1 nM R1881 (methyltrienolone, Perkin Elmer). For anti-androgen treatment, 10 µM bicalutamide (Astra Zeneca) was added to the medium 30 min before R1881 stimulation. To block protein synthesis, 25 µg/ml cycloheximide (Sigma-Aldrich) was added to the medium at the same time as R1881.

RNA extraction. Total RNA was extracted from cells and tissue samples using TriPURE Isolation Reagent (ROCHE).

Quantification of mature miR-135a by RT-qPCR. The reverse transcription (RT) reactions were performed, using TaqMan® microRNA RT Kit and TaqMan® small RNA primers assays (Applied Biosystems), with 200 or 10 ng total RNA for miR-135a or U6 snRNA, respectively. QPCR were performed with noUNG TaqMan® Universal PCR Master mix (Applied Biosystems). MiR-135a expression was normalized relative to U6 snRNA expression level. For tissue samples, RT reactions were performed with 10 ng total RNA and miR-135a expression was normalized relative to the RNU24 expression. Relative quantification was done using the $2^{-\Delta\Delta Ct}$ formula.

Quantification of pri-miR and mRNA by RT-qPCR. cDNA was synthesized from 1 µg of total RNA treated with DNAseI, using the First-Strand cDNA Synthesis kit (Life Technologies). QPCR were performed using QuantiTect SYBR Green PCR kit (Qiagen) and primers listed in **supplementary Table 1**. Values were normalized by the median of housekeeping genes expression (TBP, RPS17, RPLP0; QuantiTect Primers, Qiagen). Relative quantification was done using the $2^{-\Delta\Delta Ct}$ formula.

5'RACE. RNA (1 µg) extracted from LNCaP cells with RNeasy mini kit (Qiagen) was used to determine the Transcription Start Site of pri-miR-135a2, using SuperscriptIII RT (55°C) and the 5'RACE system for rapid amplification of cDNA ends (Life Technologies, primers listed in **supplementary Table 1**). The PCR product was cloned by TA cloning in pGEM-Teasy (Promega) and sequenced.

Functional ARE identification by luciferase reporter assay. Fragments upstream of the miR-135a2 genomic location were amplified by PCR from LNCaP genomic DNA (primers listed in **supplementary Table 1)** and cloned into the pGL3-promoter vector (Promega). Two point mutations in the ARE-2 were inserted using the QuikChange II XL site-directed mutagenesis kit (Stratagene). Luciferase reporter assay was done, as previously described (48).

Chromatin immunoprecipitation (ChIP). ChIP assay was done in LNCaP cells as previously described (48). Primers used for qPCR are listed in **supplementary Table 1**.

miRNA, miRNA inhibitor, siRNA and plasmid transfections. miRNA mimics (50 nM miR-135a or miR-NC negative control#2; Applied Biosystems), pCAGmycROCK1 (a gift

from MF Olson) and pmirGLO were transfected into cells using Lipofectamine2000 (Life Technologies). siRNA anti-AR, anti-ROCK1, anti-ROCK2 or si-Non Targeting (si-NT) (50 nM ON-TARGET*plus* SMARTpool, Dharmacon) and miR-135a inhibitor (25 nM miRCURY LNA Power Inhibitor, Exiqon) were transfected into cells using DharmaFECT (Dharmacon).

Western Blot. 50 µg of proteins were analyzed by western blotting, using anti-ROCK1 (GTX113266, 1:500, GeneTex), anti-ROCK2 (sc-1851, 1:200, Santa Cruz) and anti-β-tubulin (T4026, 1:4 000, Sigma-Aldrich) antibodies. Protein expression was quantified with MultiGauge software and normalized to β-Tubulin expression.

Luciferase reporter assay for 3'UTR/miR interaction. The 3'UTR of human *ROCK1* (nt 1-920) and *ROCK2* (nt 1-816) were amplified by PCR from LNCaP genomic DNA (primers listed in **supplementary Table 1**) and cloned downstream of the Firefly luciferase gene in the pmirGLO vector (Promega). The miR-135a binding sites were then deleted by PCR. 6 x 10^4 HeLa cells seeded in 24-well plates were transfected with 200 ng of pmirGLO constructs and miRNA mimics. Two days later, cells were lysed and Firefly/Renilla luciferase activities were determined using the Dual Luciferase Assay System (Promega).

Wound Healing migration assay. PC-3 cells were transfected with miRNA mimics, siRNA or treated with 16 µg/ml of Y-27632 (Sigma-Aldrich). Two days later, wounds were formed by scraping across cell monolayer using a micropipette tip. Phase contrast photomicrographs were recorded at 5 min intervals until 48 h, using a time-lapse microscope (Axiovert100M, Zeiss). The speed of wound closure was measured with ImageJ software. For ROCK1 rescue, 2 µg of pCAGmycROCK1 were transfected 24 h after miRNA mimics transfection.

Matrigel invasion chamber assay. PC-3 cells were transfected with miRNA mimics, siRNA or treated with 16 µg/ml of Y-27632 and cultured 48 h in serum free medium containing 1% BSA. Cells were labeled 1 h at 37°C with 10 µg/ml $DiIC_{12}(3)$ (BD Biosciences) and seeded for 30 h into fluoroblock insert (8 µm pore size) with GFR (Growth Factors Reduced)-Matrigel coated-membrane or not (BD Biosciences), placed in well containing 10% serum medium. Data were expressed as percentage of invasive relative to migrating cells. For ROCK1 rescue, 2 µg of pCAGmycROCK1 were transfected 24 h after miRNA mimics transfection.

***In ovo* tumor growth and invasion assay.** Work using chick embryos was done under animal experimentation permits N°381029 and N°B3851610001. Fertilized white Leghorn eggs were incubated at 38°C with 60% relative humidity for 10 days. At this stage (E10), the chorioallantoic membrane (CAM) was dropped by drilling a small hole through the eggshell into the air sac and a 1 cm^2 window was cut in the eggshell above the CAM. PC-3 cells stably overexpressing miR-Null or miR-135a were labeled with VybrantTM DiO (Molecular Probes) and resuspended in serum free medium. For each condition, 10^6 cells (50 µl) were grafted onto the CAM of 35 embryos, before the eggs were returned to the incubator. At E19, the upper portion of the CAM was removed, transferred in PBS, then the tumors were cut away from normal CAM tissue and weighted. In parallel, a 1 cm^2 portion of the lower CAM was collected and fixed in 4% formaldehyde in PBS to evaluate the number of invasive nodules, using a Leica Macrofluo fluorescent microscope.

Xenograft studies in mice. Experiments were performed in compliance with the French Guidelines for care and use of experimental animals and approved by the ethical committee CECCAPP (C2EA-15) of the Ecole Normale Supérieure de Lyon. Stably genetically modified PC-3 cells (10^6 cells overexpressing miR-Null or miR-135a in 150 µl PBS) were injected

subcutaneously on the left flank of 8 weeks old male SCID mice. After 6 weeks post-xenograft, animals were sacrificed by cervical dislocation, dissected and tumors collected.

Human tissue samples. Prostate tissue with adenocarcinoma and normal adjacent counterpart were obtained from 56 patients who underwent radical prostatectomy. None of the patients had received preoperative chemotherapy or radiation therapy. Clinical informations for patients are summarized in **supplementary Tables 2-3**.

Immunohistochemistry (IHC) on tissue samples. 3 µm-thick tissue sections were prepared from 56 paraffin embedded human prostate tissue samples. Immunohistochemical staining with anti-ROCK1 antibody (GTX113266, 1:80, GeneTex) was performed on the Ventana Benchmark Ultra XT automated stainer, using the ultraview DAB detection kit (Ventana).

Statistical analysis. Statistical analyses were conducted using GraphPad Prism 5 software. A p-value < 0.05 was considered as statistically significant.

Disclosure of Potential Conflicts of interest

The authors declare no conflicts of interest.

Acknowledgements

Work was supported by grants from Institut Mérieux and the Ligue Contre le Cancer. Authors thank Julien DUGAS (CarMen Lab) for his contribution in statistical analyses, Céline MICHAUX, Karine CASTELLANO and Béatrice BANCEL (Service d'Anatomie et Cytologie Pathologiques, Hospices Civils de Lyon) for providing patient samples and performing IHC staining, Jean VIALLET for performing *in ovo* assay, Christophe CHAMOT and Claire LIONNET (Microscopy core facility) and Patrick Manas (AniRA-PBES platform) of UMS3444/US8 SFR Biosciences Gerland-Lyon Sud, for assistance in wound healing assay and performing xenograft assay in mice, respectively.

References

1. Cunha GR, Ricke W, Thomson A, Marker PC, Risbridger G, Hayward SW, et al. Hormonal, cellular, and molecular regulation of normal and neoplastic prostatic development. The Journal of steroid biochemistry and molecular biology. 2004;92(4):221-36.
2. Matsumoto T, Sakari M, Okada M, Yokoyama A, Takahashi S, Kouzmenko A, et al. The androgen receptor in health and disease. Annu Rev Physiol. 2013;75:201-24.
3. Green SM, Mostaghel EA, Nelson PS. Androgen action and metabolism in prostate cancer. Mol Cell Endocrinol. 2012;360(1-2):3-13.
4. Denayer S, Helsen C, Thorrez L, Haelens A, Claessens F. The rules of DNA recognition by the androgen receptor. Molecular endocrinology. 2010;24(5):898-913.
5. Chen Y, Clegg NJ, Scher HI. Anti-androgens and androgen-depleting therapies in prostate cancer: new agents for an established target. The lancet oncology. 2009;10(10):981-91.
6. Feldman BJ, Feldman D. The development of androgen-independent prostate cancer. Nature reviews Cancer. 2001;1(1):34-45.
7. Knudsen KE, Penning TM. Partners in crime: deregulation of AR activity and androgen synthesis in prostate cancer. Trends Endocrinol Metab. 2010;21(5):315-24.
8. Takayama KI, Inoue S. Transcriptional network of androgen receptor in prostate cancer progression. Int J Urol. 2013;20(8):756-68.
9. Bartel DP. MicroRNAs: target recognition and regulatory functions. Cell. 2009;136(2):215-33.
10. Esquela-Kerscher A, Slack FJ. Oncomirs - microRNAs with a role in cancer. Nature reviews Cancer. 2006;6(4):259-69.
11. Xi JJ. MicroRNAs in Cancer. Cancer treatment and research. 2013;158:119-37.
12. Jansson MD, Lund AH. MicroRNA and cancer. Molecular oncology. 2012;6(6):590-610.
13. Hurst DR, Edmonds MD, Welch DR. Metastamir: the field of metastasis-regulatory microRNA is spreading. Cancer research. 2009;69(19):7495-8.
14. Bouyssou JM, Manier S, Huynh D, Issa S, Roccaro AM, Ghobrial IM. Regulation of microRNAs in Cancer Metastasis. Biochimica et biophysica acta. 2014.
15. Croce CM. Causes and consequences of microRNA dysregulation in cancer. Nature reviews Genetics. 2009;10(10):704-14.
16. Fang YX, Gao WQ. Roles of microRNAs during prostatic tumorigenesis and tumor progression. Oncogene. 2014;33(2):135-147.
17. Watahiki A, Wang Y, Morris J, Dennis K, O'Dwyer HM, Gleave M, et al. MicroRNAs associated with metastatic prostate cancer. PloS one. 2011;6(9):e24950.
18. Hassan O, Ahmad A, Sethi S, Sarkar FH. Recent updates on the role of microRNAs in prostate cancer. J Hematol Oncol. 2012;5:9.
19. Fendler A, Stephan C, Yousef GM, Jung K. MicroRNAs as regulators of signal transduction in urological tumors. Clinical chemistry.57(7):954-68.
20. Ribas J, Ni X, Haffner M, Wentzel EA, Salmasi AH, Chowdhury WH, et al. miR-21: an androgen receptor-regulated microRNA that promotes hormone-dependent and hormone-independent prostate cancer growth. Cancer research. 2009;69(18):7165-9.
21. Jalava SE, Urbanucci A, Latonen L, Waltering KK, Sahu B, Janne OA, et al. Androgen-regulated miR-32 targets BTG2 and is overexpressed in castration-resistant prostate cancer. Oncogene. 2012;31(41):4460-71.

22. Fletcher CE, Dart DA, Sita-Lumsden A, Cheng H, Rennie PS, Bevan CL. Androgen-regulated processing of the oncomir miR-27a, which targets Prohibitin in prostate cancer. Human molecular genetics. 2012;21(14):3112-27.
23. Sun D, Layer R, Mueller AC, Cichewicz MA, Negishi M, Paschal BM, et al. Regulation of several androgen-induced genes through the repression of the miR-99a/let-7c/miR-125b-2 miRNA cluster in prostate cancer cells. Oncogene. 2014;33(11):1448-57.
24. Waltering KK, Porkka KP, Jalava SE, Urbanucci A, Kohonen PJ, Latonen LM, et al. Androgen regulation of micro-RNAs in prostate cancer. The Prostate. 2011;71(6):604-14.
25. Ambs S, Prueitt RL, Yi M, Hudson RS, Howe TM, Petrocca F, et al. Genomic profiling of microRNA and messenger RNA reveals deregulated microRNA expression in prostate cancer. Cancer research. 2008;68(15):6162-70.
26. Murata T, Takayama K, Katayama S, Urano T, Horie-Inoue K, Ikeda K, et al. miR-148a is an androgen-responsive microRNA that promotes LNCaP prostate cell growth by repressing its target CAND1 expression. Prostate cancer and prostatic diseases. 2010;13(4):356-61.
27. Amano M, Nakayama M, Kaibuchi K. Rho-kinase/ROCK: A key regulator of the cytoskeleton and cell polarity. Cytoskeleton (Hoboken). 2010;67(9):545-54.
28. Riento K, Ridley AJ. Rocks: multifunctional kinases in cell behaviour. Nat Rev Mol Cell Biol. 2003;4(6):446-56.
29. Somlyo AV, Bradshaw D, Ramos S, Murphy C, Myers CE, Somlyo AP. Rho-kinase inhibitor retards migration and in vivo dissemination of human prostate cancer cells. Biochemical and biophysical research communications. 2000;269(3):652-9.
30. Golubovskaya VM, Sumbler B, Ho B, Yemma M, Cance WG. MiR-138 and MiR-135 directly target focal adhesion kinase, inhibit cell invasion, and increase sensitivity to chemotherapy in cancer cells. Anti-cancer agents in medicinal chemistry. 2014;14(1):18-28.
31. Shin JY, Kim YI, Cho SJ, Lee MK, Kook MC, Lee JH, et al. MicroRNA 135a Suppresses Lymph Node Metastasis through Down-Regulation of ROCK1 in Early Gastric Cancer. PloS one. 2014;9(1):e85205.
32. Chen Y, Zhang J, Wang H, Zhao J, Xu C, Du Y, et al. miRNA-135a promotes breast cancer cell migration and invasion by targeting HOXA10. BMC Cancer. 2012;12:111.
33. Zhou W, Li X, Liu F, Xiao Z, He M, Shen S, et al. MiR-135a promotes growth and invasion of colorectal cancer via metastasis suppressor 1 in vitro. Acta Biochim Biophys Sin (Shanghai). 2012;44(10):838-46.
34. Leung CO, Deng W, Ye TM, Ngan HY, Tsao GS, Cheung AN, et al. Mir-135a leads to cervical cancer cell transformation through regulation of ss-catenin via a siah1-dependent ubiquitin proteosomal pathway. Carcinogenesis. 2014.
35. Ma S, Chan YP, Kwan PS, Lee TK, Yan M, Tang KH, et al. MicroRNA-616 induces androgen-independent growth of prostate cancer cells by suppressing expression of tissue factor pathway inhibitor TFPI-2. Cancer research. 2011;71(2):583-92.
36. Wang G, Wang Y, Feng W, Wang X, Yang JY, Zhao Y, et al. Transcription factor and microRNA regulation in androgen-dependent and -independent prostate cancer cells. BMC genomics. 2008;9 Suppl 2:S22.
37. DeVere White RW, Vinall RL, Tepper CG, Shi XB. MicroRNAs and their potential for translation in prostate cancer. Urologic oncology. 2009;27(3):307-11.
38. Zheng C, Yinghao S, Li J. MiR-221 expression affects invasion potential of human prostate carcinoma cell lines by targeting DVL2. Medical oncology. 2012;29(2):815-22.
39. Sun D, Lee YS, Malhotra A, Kim HK, Matecic M, Evans C, et al. miR-99 family of MicroRNAs suppresses the expression of prostate-specific antigen and prostate cancer cell proliferation. Cancer research. 2011;71(4):1313-24.

40. Li Y, Kong D, Ahmad A, Bao B, Dyson G, Sarkar FH. Epigenetic deregulation of miR-29a and miR-1256 by isoflavone contributes to the inhibition of prostate cancer cell growth and invasion. Epigenetics. 2012;7(8):940-9.
41. Nadiminty N, Tummala R, Lou W, Zhu Y, Shi XB, Zou JX, et al. MicroRNA let-7c is downregulated in prostate cancer and suppresses prostate cancer growth. PloS one. 2012;7(3):e32832.
42. Takayama K, Tsutsumi S, Katayama S, Okayama T, Horie-Inoue K, Ikeda K, et al. Integration of cap analysis of gene expression and chromatin immunoprecipitation analysis on array reveals genome-wide androgen receptor signaling in prostate cancer cells. Oncogene. 2011;30(5):619-30.
43. Cao P, Deng Z, Wan M, Huang W, Cramer SD, Xu J, et al. MicroRNA-101 negatively regulates Ezh2 and its expression is modulated by androgen receptor and HIF-1alpha/HIF-1beta. Molecular cancer. 2010;9:108.
44. Wen S, Shang Z, Zhu S, Chang C, Niu Y. Androgen receptor enhances entosis, a non-apoptotic cell death, through modulation of Rho/ROCK pathway in prostate cancer cells. The Prostate. 2013;73(12):1306-15.
45. Gonzalez-Montelongo MC, Marin R, Gomez T, Marrero-Alonso J, Diaz M. Androgens induce nongenomic stimulation of colonic contractile activity through induction of calcium sensitization and phosphorylation of LC20 and CPI-17. Molecular endocrinology. 2010;24(5):1007-23.
46. Wang BD, Yang Q, Ceniccola K, Bianco F, Andrawis R, Jarrett T, et al. Androgen receptor-target genes in african american prostate cancer disparities. Prostate cancer. 2013;2013:763569.
47. Rao S, Lyons LS, Fahrenholtz CD, Wu F, Farooq A, Balkan W, et al. A novel nuclear role for the Vav3 nucleotide exchange factor in androgen receptor coactivation in prostate cancer. Oncogene. 2012;31(6):716-27.
48. Allioli N, Vincent S, Vlaeminck-Guillem V, Decaussin-Petrucci M, Ragage F, Ruffion A, et al. TM4SF1, a novel primary androgen receptor target gene over-expressed in human prostate cancer and involved in cell migration. The Prostate. 2011;71(11):1239-50.
49. Chalmel F, Primig M. The Annotation, Mapping, Expression and Network (AMEN) suite of tools for molecular systems biology. BMC Bioinformatics. 2008;9:86.
50. Bouhallier F, Allioli N, Lavial F, Chalmel F, Perrard MH, Durand P, et al. Role of miR-34c microRNA in the late steps of spermatogenesis. RNA. 2010;16(4):720-31.

Legends to Figures

Figure 1. Androgen regulation of miR-135a expression in LNCaP cells.

Mature miR-135a expression or pri-miR-135a was quantified by RT-qPCR. Results are presented as the means ± SD of three independent experiments.

A. Kinetics of miR-135a expression in LNCaP cells treated with 1 nM R1881 compared to vehicle-treated cells.

B. MiR-135a expression level in LNCaP cells treated with either 10 µM bicalutamide, 1 nM R1881 or both, relative to vehicle-treated cells.

C. MiR-135a expression level in LNCaP cells, following 48 h transfection of 50 nM siRNA against AR (si-AR) or non-targeting siRNA (si-NT) and 24 h of 1 nM R1881 or vehicle treatment.

D. MiR-135a expression in LNCaP cells treated with either 25 µg/ml cycloheximide, 1 nM R1881 or both, relative to vehicle-treated cells.

E. Pri-miR-135a1 and 135a2 expression in LNCaP cells treated during 24 h with 1 nM R1881 relative to vehicle-treated cells.

F. Kinetics of pri-miR-135a2 and mature miR-135a expression in LNCaP cells treated with 1 nM R1881 relative to vehicle-treated cells.

Figure 2. Characterization of transcriptional regulation elements in miR-135a2 locus.

A. Schematic illustration of *miR-135a2* genomic region. The transcription start site (TSS), corresponding to the start of the pri-miR-135a2, was identified by 5'RACE and is represented by an arrow. The sequence of an Expressed Sequence Tag (EST), starting at the same location as TSS, was found in BLAST analysis and is represented flanked by two brackets. The sequences of the pre-miR-135a2 (underlined) and of the miR mature (surrounded) were recovered from miRBase with accession number MI0000453.

B. Schematic locations of the *in silico*-identified AREs upstream of the pre-miR-135a2. The sequence of the ARE-2 in grey circle is the closest to the ARE consensus sequence.

C. Responsiveness to the ligand-stimulated AR of potential AREs identified upstream of the miR-135a2 locus assessed by luciferase reporter assays. HeLa cells were co-transfected with pSG5-hAR and pGL3-promoter constructs containing the potential AREs cloned upstream of the minimal promoter SV40. The ARE-2 is represented in grey. One construct contains an ARE-2 mutant represented by a grey barred circle. Cells were treated with 1 nM R1881 or vehicle for 24 h before harvesting for reporter analyses. Results are shown as luciferase activity in R1881 relative to vehicle treated cells and presented as the means $\pm$ SD of three independent experiments.

D. AR binding on ARE-2 region of *miR-135a2* in LNCaP cells treated with 1 nM R1881 relative to vehicle-treated cells and determined by chromatin immunoprecipitation (ChIP). LNCaP cells were treated or not with 1 nM R1881 during 24 h, ChIP experiments were carried out using an anti-AR antibody. The precipitated DNAs were used as templates for qPCR. As controls, promoter region of *TBP* served as non-target sequence while enhancer region of the *PSA* served as known AR target sequence.

Figure 3. Androgens/AR signaling down-regulates ROCK1 and ROCK2 expression through miR-135a which binds to their 3'UTRs.

A. ROCK1 and ROCK2 mRNAs expression in LNCaP cells, 48 h after 50 nM miR-135a or miR-NC (negative control) transfection and determined by RT-qPCR.

B. Western Blot analysis of ROCK1 and ROCK2 protein expression in LNCaP cells, 48 h after 50 nM miR-135a or miR-NC transfection. The values below represent the relative abundance of the protein normalized to β-Tubulin expression.

C. Schematic representation of plasmid constructs containing ROCK1 or ROCK2 3'UTR with the putative sequences targeted by miR-135a (black square, complementary to the seed box) and the mutants deleted for miR-135a targeted sequence.

D. Interaction of miR-135a with ROCK1 and ROCK2 3'UTRs assessed by luciferase reporter assay. The pmirGLO vectors containing wild type or mutant ROCK1 or ROCK2 3'UTR were transfected into HeLa cells with miR-135a or miR-NC. Results are presented as luciferase activity in miR-135a relative to miR-NC transfected cells.

E. Western Blot analysis of ROCK1 and ROCK2 protein expression in LNCaP cells, treated during 48 h with 1 nM R1881 or vehicle (ethanol) and transfected or not at the same time with a miR-135a inhibitor. The values below represent the relative abundance of the protein normalized to β-Tubulin expression.

For panels A and D, results are presented as the means $\pm$ SD of three independent experiments.

Figure 4. miR-135a decreases migration and invasion abilities *via* ROCK pathway.

A. Time-lapse microscopy analysis of cell migration. PC-3 cells, transfected with either miR-NC, miR-135a, siROCK1 and siROCK2 (siROCK1/2) or miR-135a and ROCK1 cDNA or treated with Y-27632 were analysed by video-microscopy in wound healing assays. In the upper panel, the speed of wound closure was expressed as percentage relative to the one in miR-NC transfected cells. In the lower panel, representative pictures of wound closure are presented (Bar = 100 µm).

B. Morphology of migrating PC-3 cells. Microscopy images of PC-3 cells transfected with either miR-NC, miR-135a, siROCK1 and siROCK2 (siROCK1/2) or miR-135a and ROCK1 cDNA or treated with Y-27632. The white arrows show cells with protrusions. Bar = 50 µm.

C. Matrigel invasion assay on PC-3 cells transfected with either miR-NC, miR-135a, siROCK1, siROCK2 or miR-135a and ROCK1, or treated with Y-27632. In the left panel, the percentage of invasive cells (determined as described in material and methods) was expressed relative to the one in miR-NC transfected cells. In the right panel, representative pictures of cells invading through matrigel under some conditions (Bar = 100 µm).

Figure 5. miR-135a overexpression inhibits *in vivo* invasion abilities of prostate PC-3 cells.

A. Quantification of nodules observed in the lower chorioallantoic membrane (CAM) of chick embryos grafted with miR-Null or miR-135a overexpressing PC-3 cells. Fluorescent labeled PC-3 cells stably overexpressing miR-Null or miR-135a were grafted onto the CAM of 10 days chick embryos (E10). At E19, a quantification of fluorescent nodules observed in the lower CAM was done. Columns represent the average number of nodules per egg; error bars represent standard deviations; n, number of grafted embryos who are alive at E19; ****, p-value < 0.0001.

B. Representative images showing the intraperitoneal or subcutaneous localization of tumors developed in mice grafted with miR-Null or miR-135a overexpressing PC-3 cells, respectively. PC-3 cells stably overexpressing miR-Null or miR-135a were subcutaneously injected in the left flank of 8-weeks adult male SCID mice. After 6 weeks, animals were dissected and tumors photographed. n, number of mice who developed tumors.

Figure 6. miR-135a expression decreases with prostate cancer progression.

A. MiR-135a expression in 56 tumor and adjacent normal tissues from prostatectomy was determined by RT-qPCR. Statistical analysis was performed according to the Wilcoxon matched-pairs signed-ranks test. ****, p<0.0001.

B. miR-135a expression, determined by RT-qPCR, in 56 PCa samples (in tumor relative to paired normal tissue from the same patient) in correlation with the Gleason score**.** Statistical analysis was performed by an unpaired t-test with Welch's correction. **, $p<0.01$

C. miR-135a expression, determined by RT-qPCR, in 56 PCa samples (in tumor relative to paired normal tissue from the same patient) in correlation with the pathological stage. pT2c, cancer localized within the prostatic capsule; pT3a, cancer extension outside the prostate but without seminal vesicles (SV) invasion; pT3b, cancer extension outside the prostate with SV invasion. Statistical analyses between groups were performed using an ANOVA analysis and between each group by Tukey-Kramer's Multiple Comparison test. ns, non-significant; *, $p<0.05$; **, $p<0.01$.

D. IHC experiments were done on 56 prostate samples from patients with PCa to determine ROCK1 protein expression level. A representative picture was taken at 400 x magnification. ROCK1 staining is given by a DAB brown stain. N, normal gland; T, tumor gland.

E. ROCK1 IHC experiments were done on 56 prostate samples from patients with PCa. ROCK1 protein expression was evaluated by a semi-quantitative IHC analysis. ROCK1 staining was rated as "high", "medium" or "low" and percentage of normal or tumor glands with high, medium or low ROCK1 protein expression determined.

Figure 1

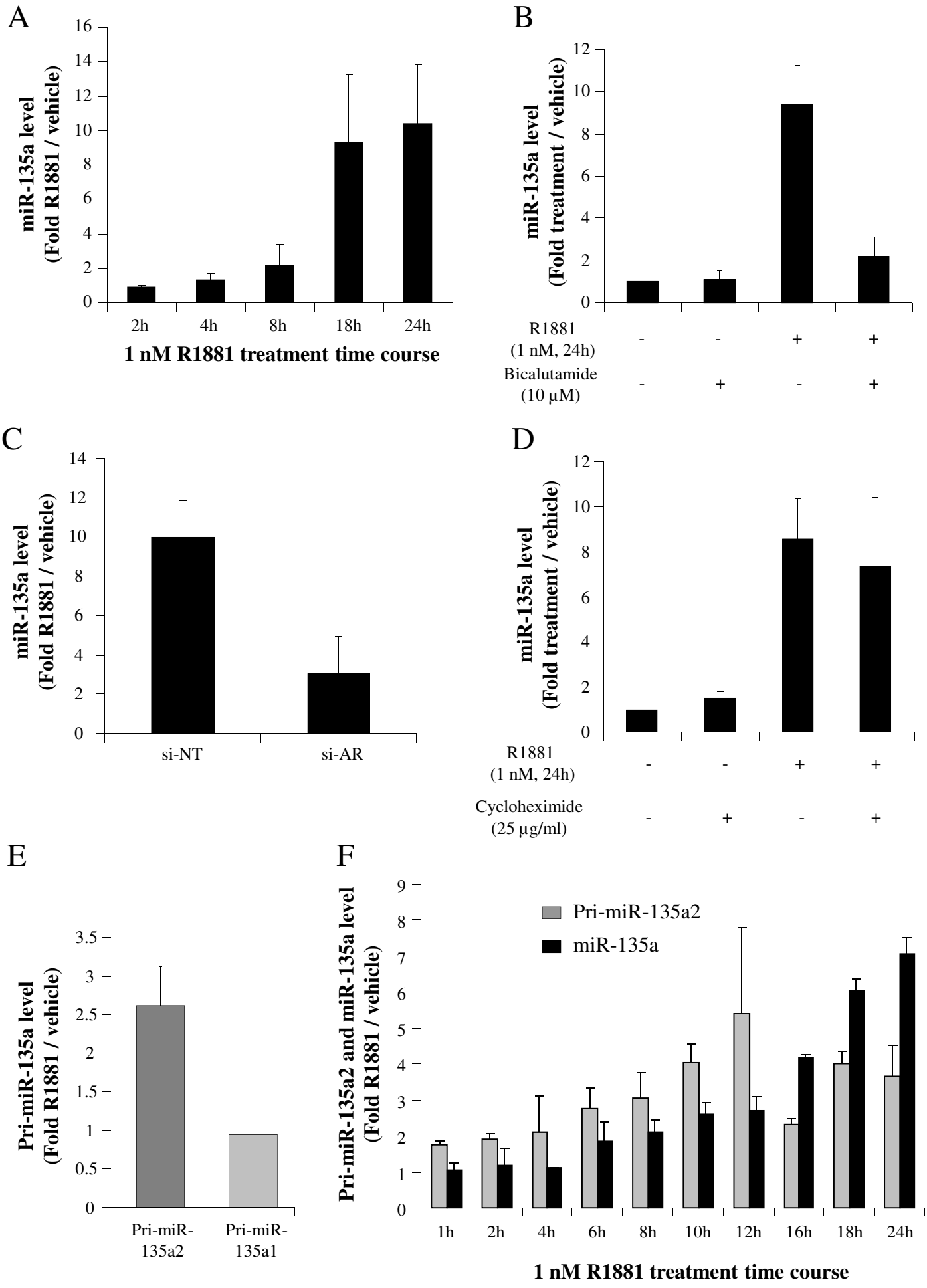
A
miR-135a level
(Fold R1881 / vehicle)
16
14
12
10
8
6
4
2
0
2h
4h
8h
18h
24h
1 nM R1881 treatment time course
B
miR-135a level
(Fold treatment / vehicle)
12
10
8
6
4
2
0
R1881
(1 nM, 24h)
- - + +
Bicalutamide
(10 μM)
- + - +
C
miR-135a level
(Fold R1881 / vehicle)
14
12
10
8
6
4
2
0
si-NT
si-AR
D
miR-135a level
(Fold treatment / vehicle)
12
10
8
6
4
2
0
R1881
(1 nM, 24h)
- - + +
Cycloheximide
(25 μg/ml)
- + - +
E
Pri-miR-135a level
(Fold R1881 / vehicle)
3.5
3
2.5
2
1.5
1
0.5
0
Pri-miR-
135a2
Pri-miR-
135a1
F
Pri-miR-135a2 and miR-135a level
(Fold R1881 / vehicle)
9
8
7
6
5
4
3
2
1
0
Pri-miR-135a2
miR-135a
1h
2h
4h
6h
8h
10h
12h
16h
18h
24h
1 nM R1881 treatment time course

Figure 2

A

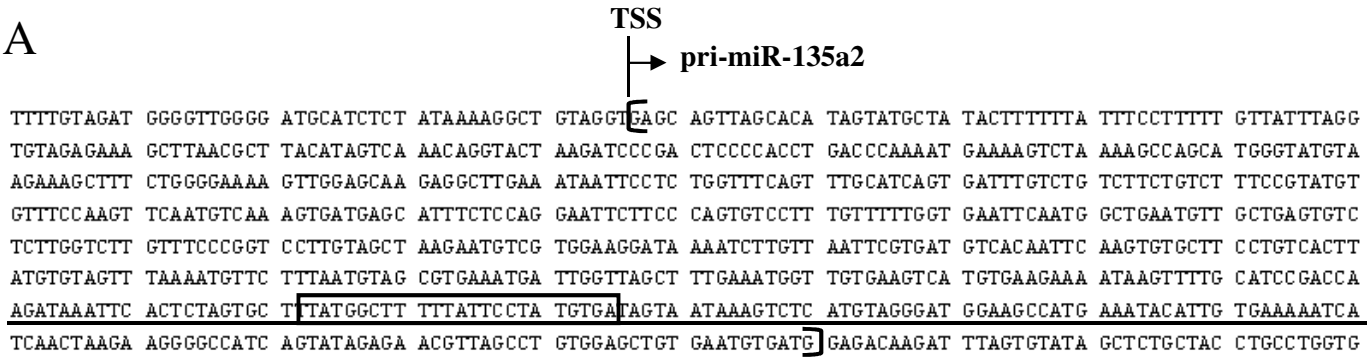

B

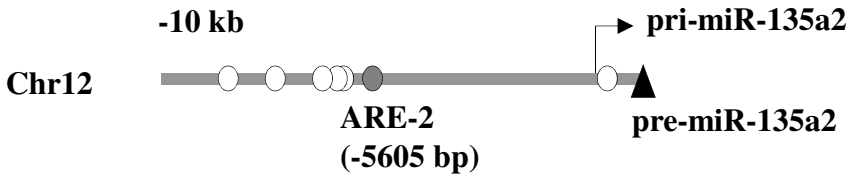

C

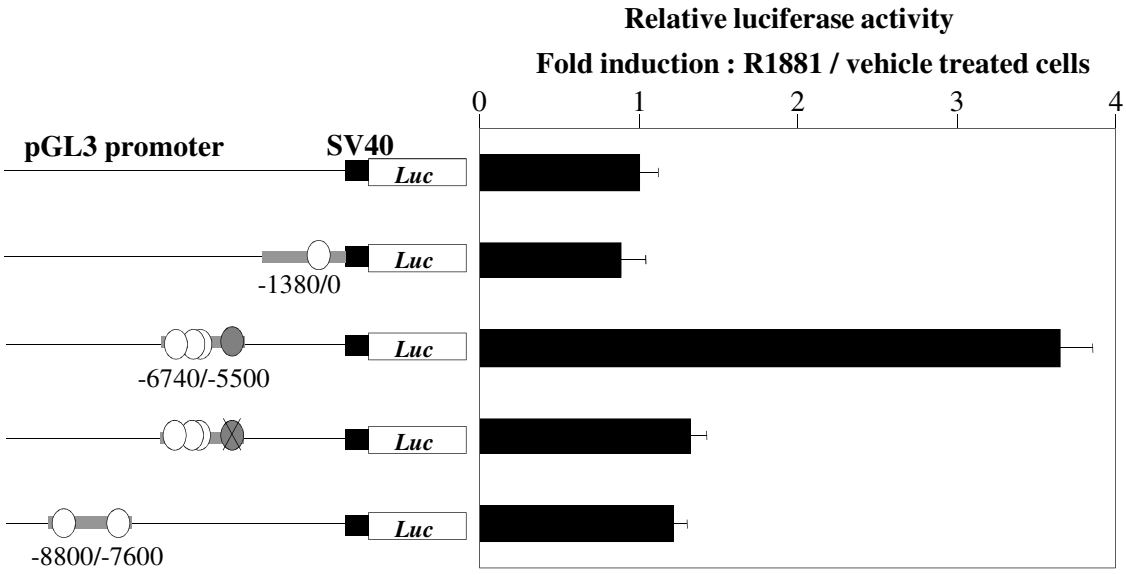

D

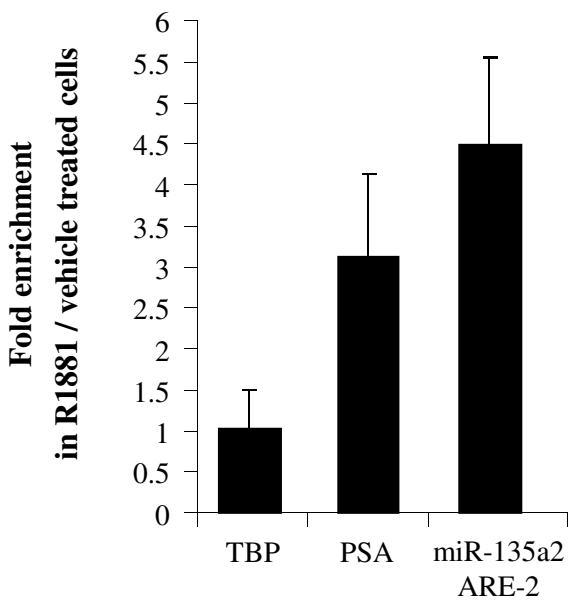

Figure 3

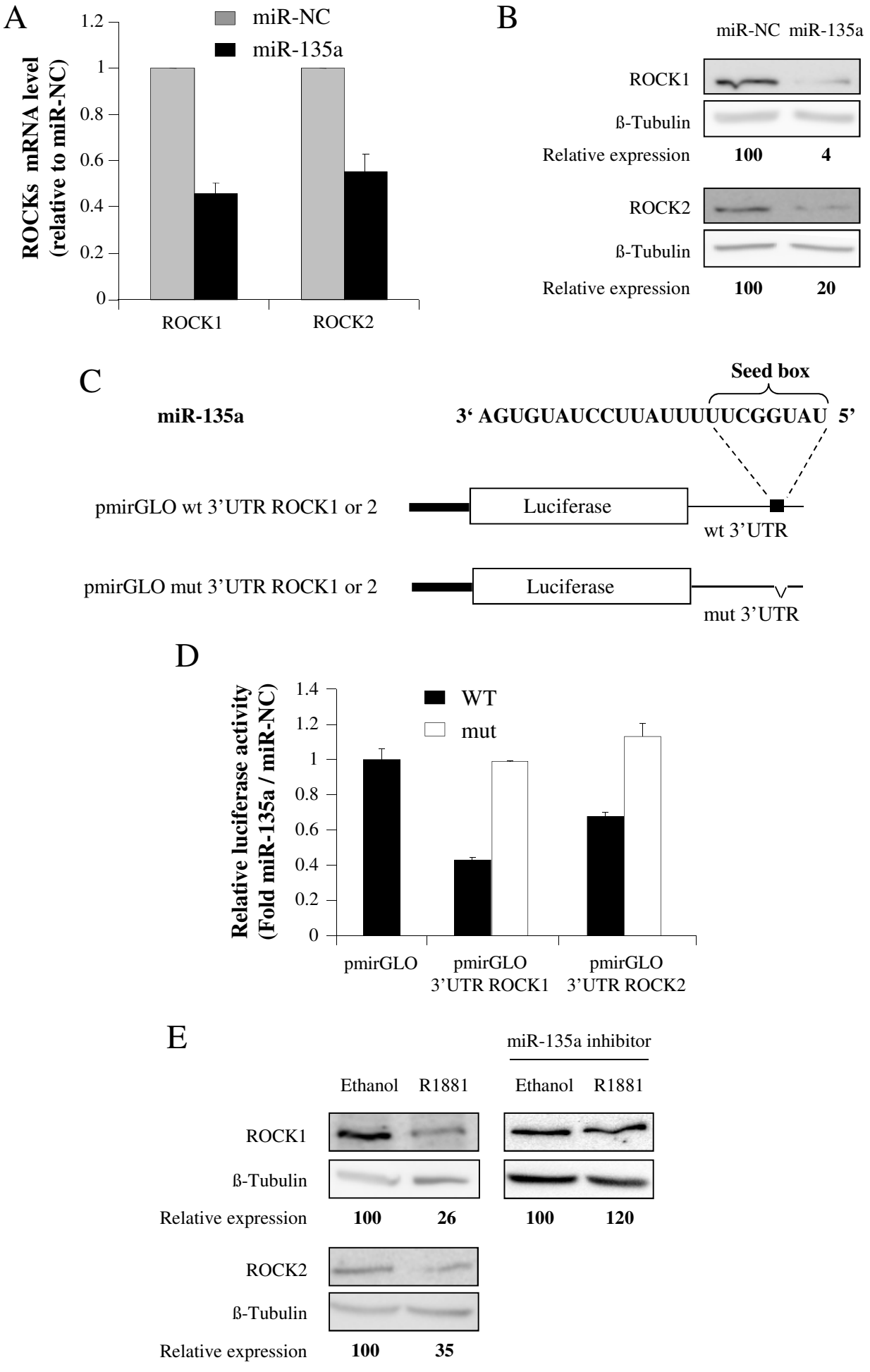
A
miR-NC
miR-135a
ROCKs mRNA level (relative to miR-NC)
1.2
1
0.8
0.6
0.4
0.2
0
ROCK1
ROCK2
B
miR-NC miR-135a
ROCK1
ß-Tubulin
Relative expression 100 4
ROCK2
ß-Tubulin
Relative expression 100 20
C
Seed box
miR-135a
3‘ AGUGUAUCCUUAUUUUUCGGUAU 5’
pmirGLO wt 3’UTR ROCK1 or 2
Luciferase
wt 3’UTR
pmirGLO mut 3’UTR ROCK1 or 2
Luciferase
mut 3’UTR
D
Relative luciferase activity (Fold miR-135a / miR-NC)
1.4
1.2
1
0.8
0.6
0.4
0.2
0
WT
mut
pmirGLO
pmirGLO 3’UTR ROCK1
pmirGLO 3’UTR ROCK2
E
miR-135a inhibitor
Ethanol R1881 Ethanol R1881
ROCK1
ß-Tubulin
Relative expression 100 26 100 120
ROCK2
ß-Tubulin
Relative expression 100 35

Figure 4

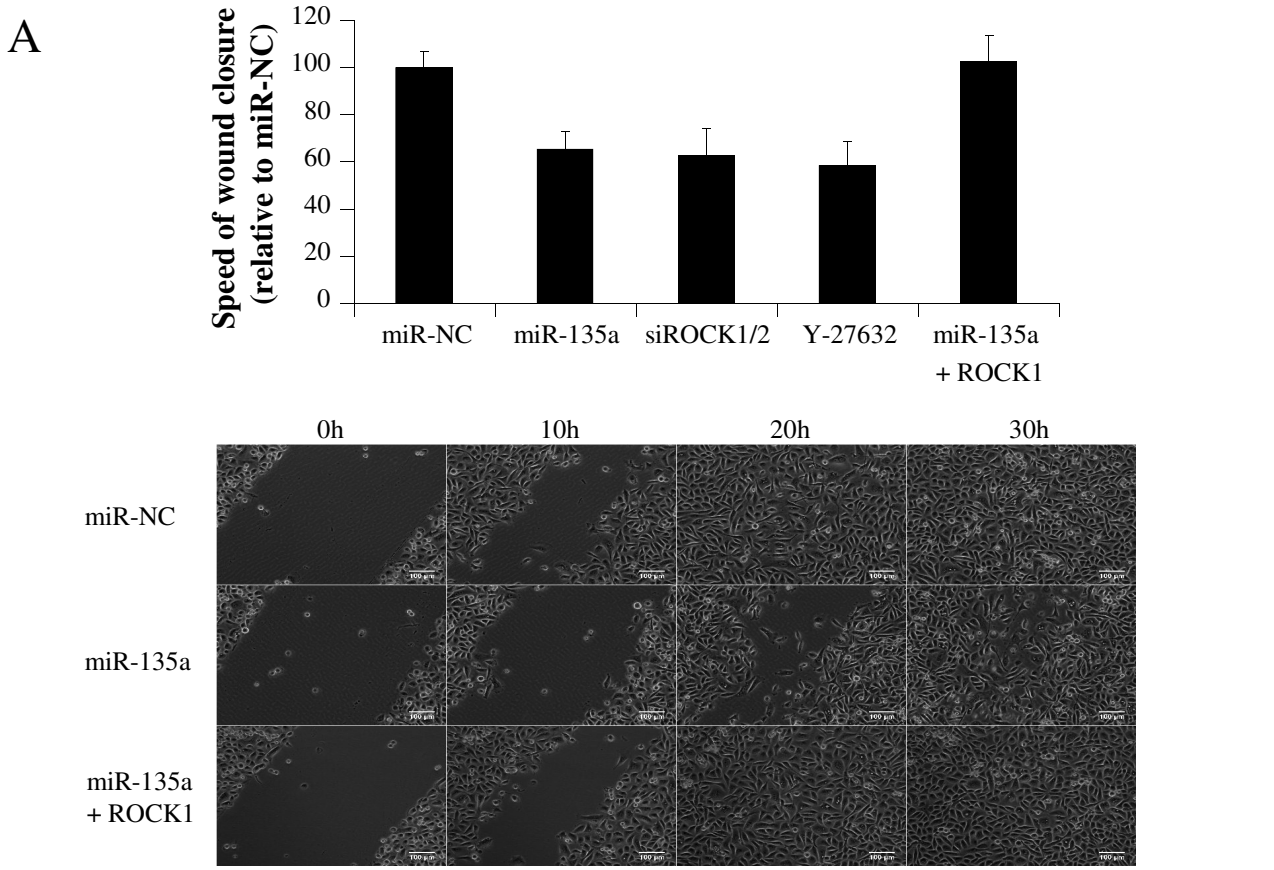
A
Speed of wound closure (relative to miR-NC)
120
100
80
60
40
20
0
miR-NC
miR-135a
siROCK1/2
Y-27632
miR-135a + ROCK1
0h
10h
20h
30h
miR-NC
miR-135a
miR-135a + ROCK1

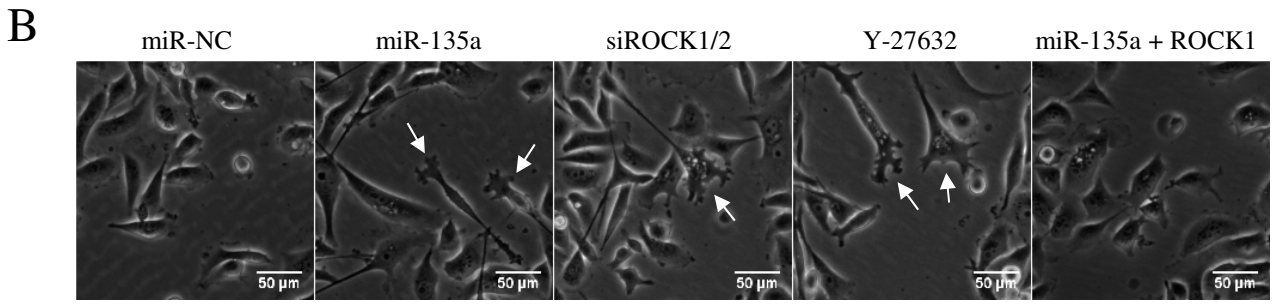
B
miR-NC
miR-135a
siROCK1/2
Y-27632
miR-135a + ROCK1
50 μm

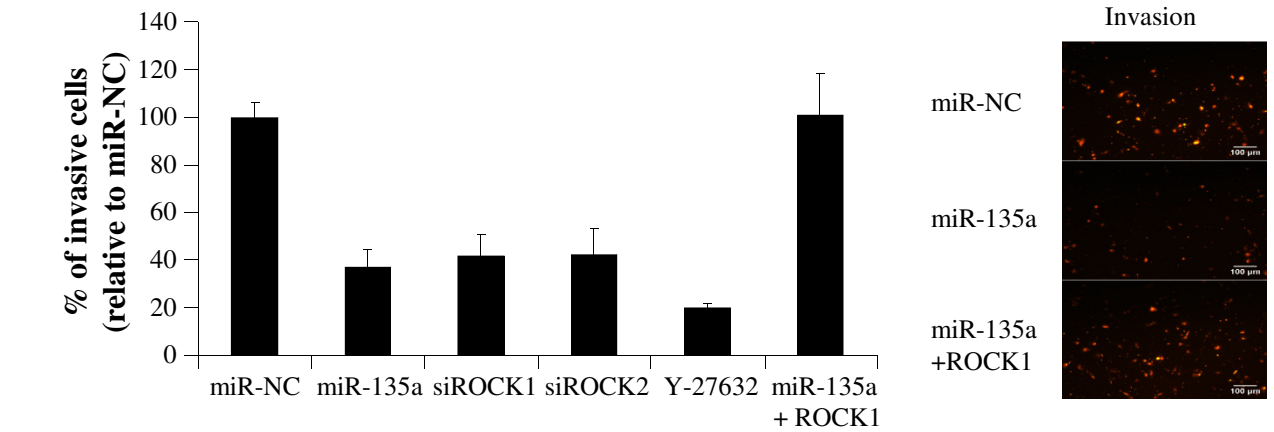
C
% of invasive cells (relative to miR-NC)
140
120
100
80
60
40
20
0
miR-NC
miR-135a
siROCK1
siROCK2
Y-27632
miR-135a + ROCK1
Invasion
miR-NC
miR-135a
miR-135a +ROCK1

Figure 5

A

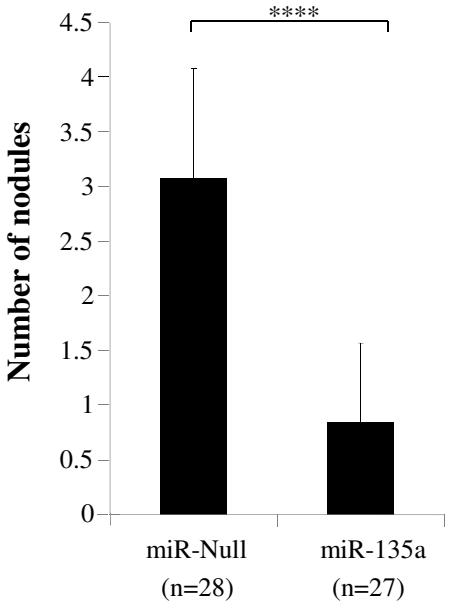
****
4.5
4
3.5
3
2.5
2
1.5
1
0.5
0
Number of nodules
miR-Null
(n=28)
miR-135a
(n=27)

B

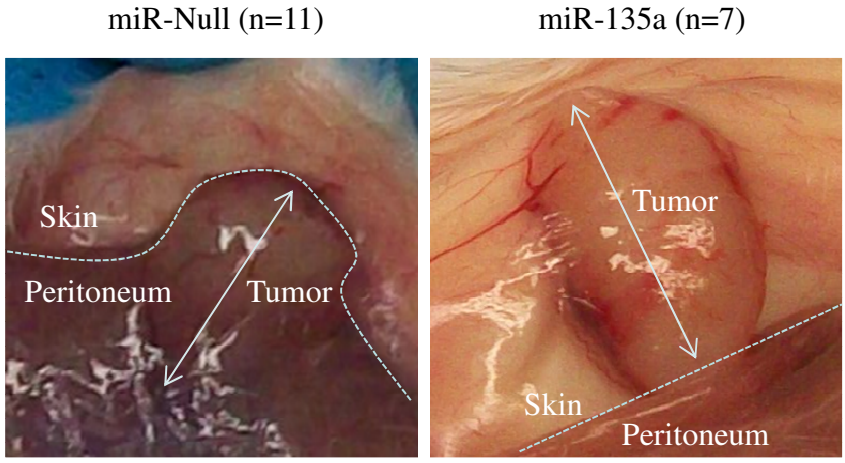
miR-Null (n=11)
miR-135a (n=7)
Skin
Peritoneum
Tumor
Tumor
Skin
Peritoneum

Figure 6

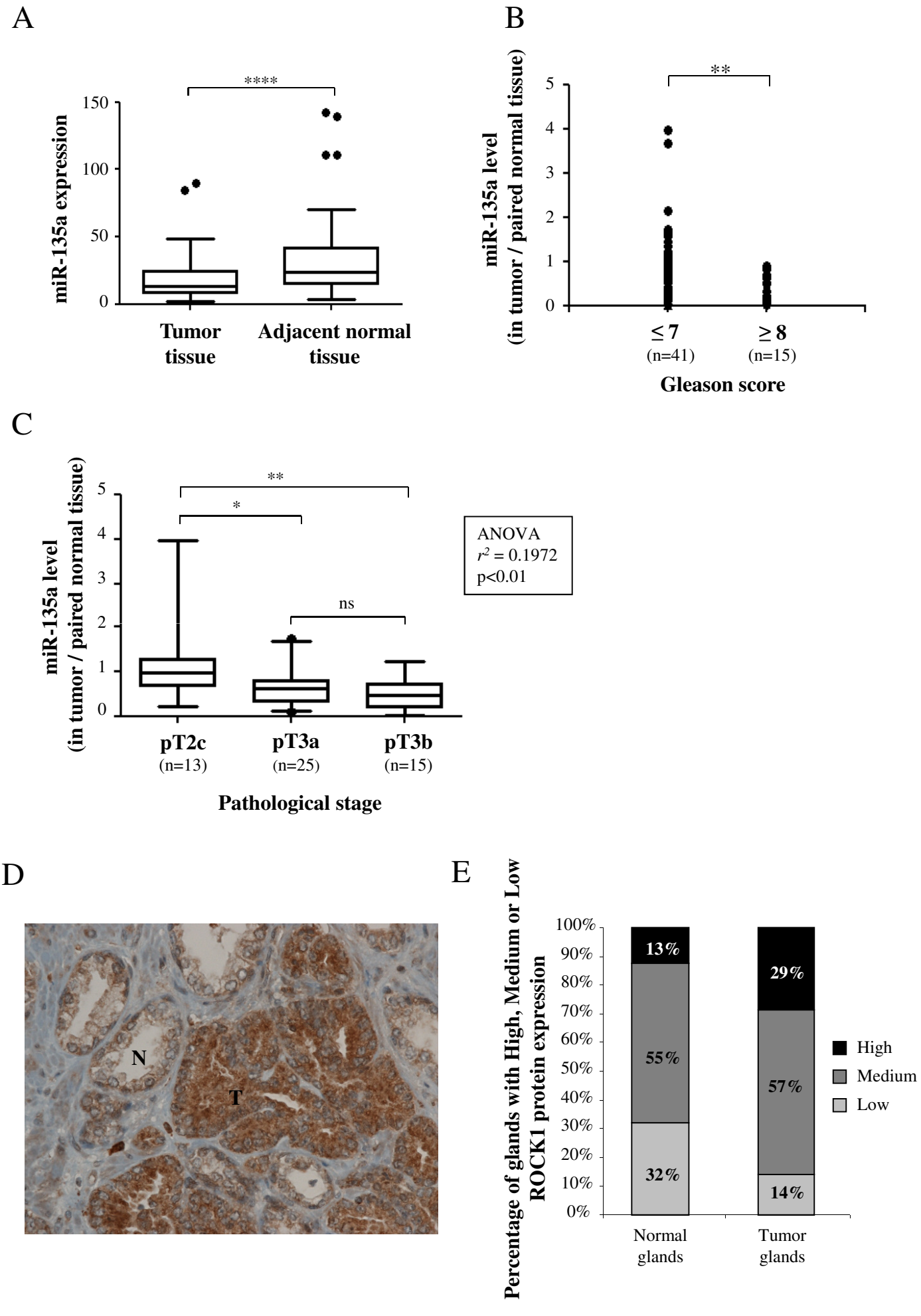
A
****
150
100
50
0
miR-135a expression
Tumor tissue
Adjacent normal tissue
B
**
5
4
3
2
1
0
miR-135a level (in tumor / paired normal tissue)
≤ 7 (n=41)
≥ 8 (n=15)
Gleason score
C
**
*
ns
5
4
3
2
1
0
miR-135a level (in tumor / paired normal tissue)
pT2c (n=13)
pT3a (n=25)
pT3b (n=15)
Pathological stage
ANOVA
r² = 0.1972
p<0.01
D
N
T
E
100%
90%
80%
70%
60%
50%
40%
30%
20%
10%
0%
Percentage of glands with High, Medium or Low ROCK1 protein expression
13%
55%
32%
29%
57%
14%
Normal glands
Tumor glands
High
Medium
Low